Supplementary material to "Influence of Surface Morphology on the Immersion Mode Ice Nucleation Efficiency of Hematite"

August 28, 2013

Naruki Hiranuma[a,*], Nadine Hoffmann[a], Alexei Kiselev[a], Axel Dreyer[b,†], Kai Zhang[c], Gourihar Kulkarni[c], Thomas Koop[b], and Ottmar Möhler[a]

[a]*Institute for Meteorology and Climate Research – Atmospheric Aerosol Research, Karlsruhe Institute of Technology, Karlsruhe, Germany.*
[b]*Faculty of Chemistry, Bielefeld University, Bielefeld, Germany.*
[†]*Now at Institute Advanced Ceramics, Hamburg University of Technology, Hamburg, Germany*
[c]*Atmospheric Science and Global Change Division, Pacific Northwest National Laboratory, Richland, Washington, USA*

*Corresponding Author. E-mail: seong.moon@kit.edu

Citation:
N. Hiranuma, N. Hoffmann, A. Kiselev, A. Dreyer, K. Zhang, G. Kulkarni, T. Koop, and O. Möhler. **Influence of Surface Morphology on the Immersion Mode Ice Nucleation Efficiency of Hematite**, for *Atmospheric Chemistry and Physics*

This supplementary information provides additional details in the measurement of absolute number of charges by polyelectrolyte titrations with PVS and PDADMAC (Table S1) as well as representative AIDA adiabatic expansion experiments (Figure S1 and S2).

Below, we briefly describe an experimental procedure to estimate maximal charge densities of hematite particles. First, we generated the maximal interface potentials in hematite suspensions by adding 0.01 mol L^{-1} NaOH or HCl solution. Compensations of the developed charges in the suspensions were directly followed and carried out by addition the oppositely charged polyelectrolyte solution (PVS or PDADMAC) to zero potential to identify the absolute number of surface charges. With measured and known parameters summarized in Table S1, we calculated the maximal charge surface densities, a (nm^{-2}), according to

$$a = \frac{c_{eq} \cdot V \cdot N_A}{m \cdot A_{BET}} \quad \text{(S1)}$$

where c_{eq} is the polyelectrolyte charge equivalent concentration (mol L^{-1}), V is the titrated volume to isoelectric point (L), N_A is the Avogadro's constant (mol^{-1}), m is the hematite mass (g) and A_{BET} is the BET specific surface area (m^2 g^{-1}). We note that 1 mol L^{-1} of polyelectrolyte concentration compensates 400 charges.

Figure S1 displays the time-series of ice crystal concentration (N_{ice}) as well as liquid droplet concentration (N_{dropet}), temperature (T), relative humidity with respect to ice and water measured by the TDL, and particle phase inferred by particles' backscattered intensities to the incident polarisation state of the laser light during the immersion mode freezing experiment for cubic hematite and milled hematite particles shown in Manuscript Figure 2 (INUIT04_13 and INUIT04_15, respectively). It is noteworthy that the observed early increases in depolarisation ratio before the full droplet formation at water saturation are the indicator of deposition mode freezing (Figure S1 A. iv. and B. iv.). As prescribed in Manuscript Section 3.2, the contributions of depositional ice formation to the total ice crystals formed through an expansion (up to 27%) was quantitatively minor and did not inhibit new ice formation in the immersion mode after reaching to the water supersaturation condition (i.e. no indication of water depletion until homogeneous freezing emerges). Therefore, the ice crystals formed through deposition mode freezing were simply subtracted from the total number of ice crystals measured within heterogeneous freezing regime to compute n_s solely accounting for the immersion mode ice nucleation.

Figure S2 illustrates the size distributions of particles, droplets, and ice crystals measured by the welas. Observed size growth at 100 s was triggered by droplet formation. Particles above 20 µm diameter were counted as ice crystals. The contributions from homogeneous ice nucleation appear below -35 ºC. Soon after that point, abrupt increase in depolarisation ratio and quick decease in water saturation were observed, which implies the presence of pure ice cloud (Figure S1).

Table S1. Summary of parameters used to calculate the charge densities, a (nm^{-2}), of cubic and miled hematite particles. PVS and PDADMAC solutions were used to obtain maximal positive and maximal negative charge densities, respectively.

Hematite	c_{eq}, 10^{-5} mol L^{-1}	V, 10^{-3} L	m, 10^{-3} g	A_{BET}, m^2 g^{-1}	a, nm^{-2}
Cubic (max. positive)	1±0.009	1.91±0.01	10.1±0.1	2.2±0.1	0.36±0.03
Cubic (max. negative)	10±0.090	1.15±0.01	10.1±0.1	2.2±0.1	1.39±0.03
Milled (max. positive)	1±0.009	1.83±0.01	8.2±0.1	3.7±0.1	0.52±0.05
Milled (max. negative)	1±0.009	7.02±0.01	8.2±0.1	3.7±0.1	3.13±0.05

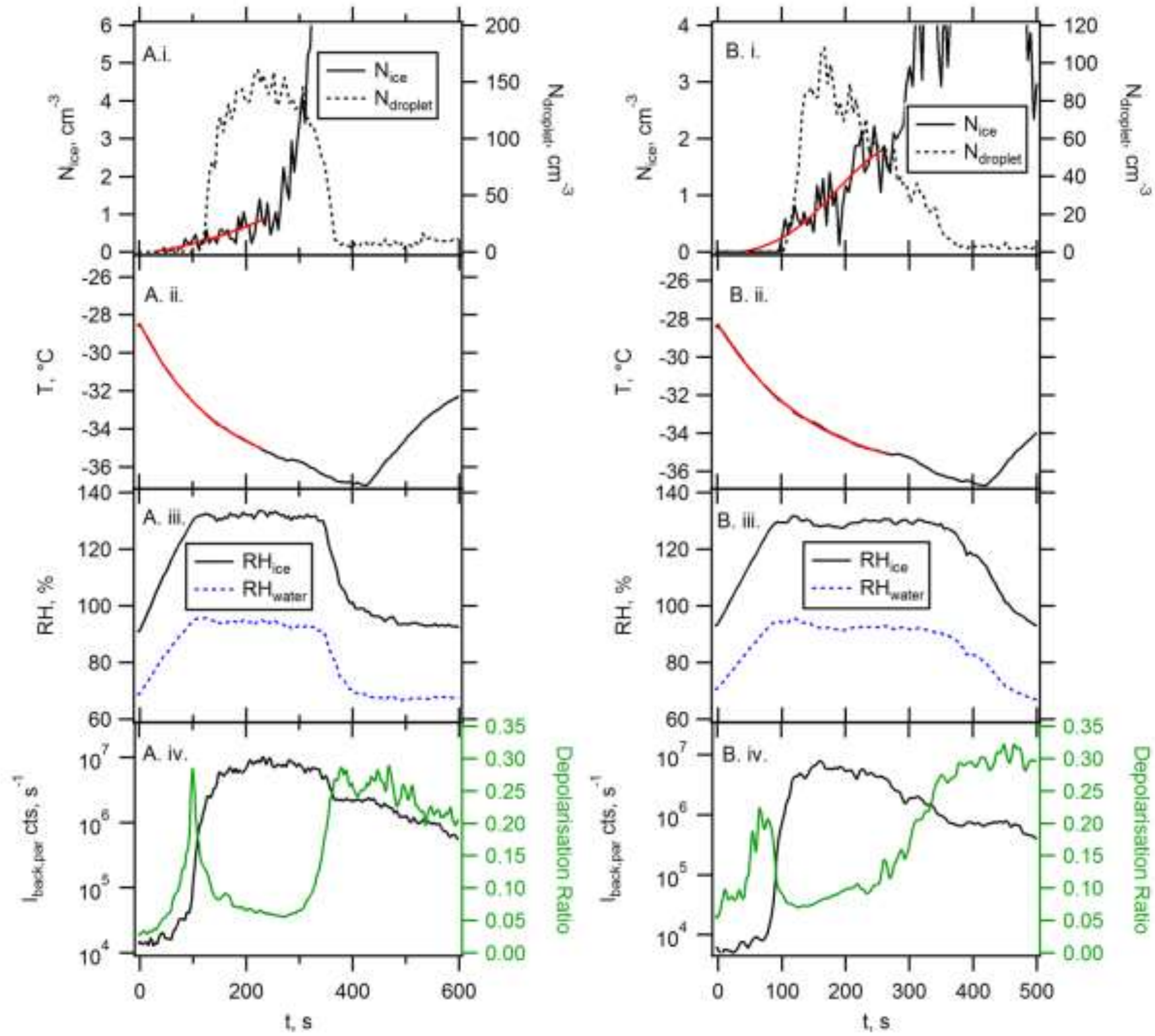

Figure S1. Typical experimental profiles, including i. ice crystal concentration (N_{ice}) and liquid droplet concentration (N_{dropet}), ii. temperature (T), iii. TDL, and iv. SIMONE measurements, of the AIDA immersion mode ice nucleation experiment for A. cubic hematite particles (INUIT04_13) and B. milled hematite particles (INUIT04_15). Note that the red lines represent interpolated data. The $I_{back,par}$ in Panel A.iv and B.iv denotes backscattered light scattering intensity parallel to the incident polarisation state (log-scaled).

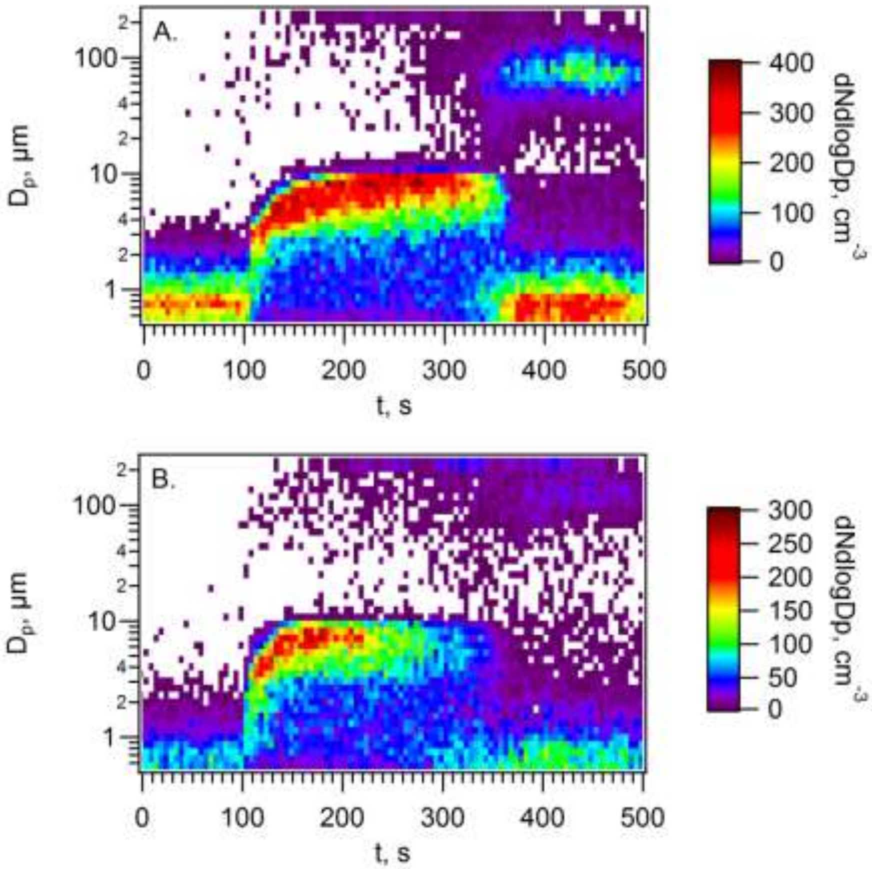

Figure S2. Time-series of the welas size distribution of the AIDA immersion mode ice nucleation experiment for A. cubic hematite particles (INUIT04_13) and B. milled hematite particles (INUIT04_15).